Chapter 4
Electrical and Physical Properties of $Sr_{0.8}Bi_{2+x}Ta_2O_{9+\delta}$ Ferroelectric Thin Films

4-1 Introduction

Ferroelectric thin films of $SrBi_2Ta_2O_9$ (SBT) have been investigated for ferroelectric random access memories applications due to their fatigue-free, and good retention characteristics, low switching field, and low leakage current. These materials belong to the family of Aurivillius compounds with a general formula $(Bi_2O_2)^{2+}(A_{m-1}B_mO_{3m+1})$, consisting of m perovskite units sandwiched between bismuth oxide layers. A variety of methods have been employed to grow SBT thin films [89-95]. Among the methods investigated, metallorganic decomposition (MOD) technique may be regarded as an interesting processing method because of its easier composition control, better homogeneity, low processing temperature, easier fabrication of large area thin films and low cost.

From previous reports [96-98], we found the ratios of Sr/Ta and Bi/Ta would affect the ferroelectrical properties of SBT films. In this study, we use MOD method to prepare SBT films containing various amounts of bismuth with constant Sr content. The inter-relationship among excess bismuth, ferroelectrical and electrical properties of the films were also investigated.

4-2 Experiment

The MOD SBT films were prepared from $Sr(CH_3COO)_2$, $Bi(CH_3COO)_3$, $Ta(OCH_2CH_3)_5$, and acetic acid as a solvent. We also added

a chelating organic ligand into the solution in order to help the formation of metal-organic compound. First, strontium acetate and bismuth acetate were dissolved in acetic acid at 120℃. Tantalum pentaethoxide was added to the solution and then the chelating agents, together refluxed for 2 h at 75℃, to produce a solution with composition of 0.8:(2+x):2 Sr:Bi:Ta ratio (x=0-1).

The SBT thin films were deposited on Ir(50nm)/ SiO_2(100nm)/Si substrates by spin-coating at 5000 rpm for 30 sec followed by pyrolysis at 150℃ for 10 min in order to evaporate the solvent, then heated at 400℃ in air for 30 min to remove other organic compounds. After repeating the process of spin coating and preheating several times, the gel films were sintered at 650℃ for 30 min with heating rate of 60℃/min in oxygen atmosphere. The thickness of SBT films is about 250 nm.

The crystallinity of SBT thin film was characterized by X-ray diffraction (XRD) with CuKα radiation at 30 kV and 20 mA. The thickness, microstructure and the surface morphology of SBT thin films were examined by field emission scanning electron microscopy (FESEM Hitachi model S4700). The P-E curve was measurement by Rt-66A. The current-voltage (I-V) measurements were performed by measuring the current through the sample with a HP 4146C semiconductor parameter analyzer. The chemical shift of bismuth was measured by x-ray photoemission spectroscopy with ESCA HPI 1600 spectrometer using an Al Kα x-ray source. The depth profiles of SBT thin films were obtained by Secondary ion mass spectroscopy (SIMS, CAMECA IMS-4f) for investigating the effects of surface layers on the electrical properties of this material. Transmission electron microscopy and energy dispersive spectroscopy (TEM-EDS, JEM-2100) which was attached with ISIS 300

energy dispersive x-ray analyzer were performed on micro-morphology of SBT thin films.

4-3 Results and discussion

The DTA and TG were used to analyze the thermal decomposition behavior of the precursor solution. The precursor solution was dried at 120 ℃ for several days. The dried powder then slowly heated in air with a ramp of 10℃/min. The weight change and heat exchange as a function of temperature were shown in Fig.4-1. From the TG data, it is seen that there is weight loss in the range 350-400℃ but almost no weight loss higher than 500℃. The DTA curve has an exothermic heat loss in the same range where the weight loss is observed. The weight loss and the exothermic peak are mainly due to the decomposition of organic groups. There is no other exothermic peak that can be attributed to the crystallization of the SBT gel.

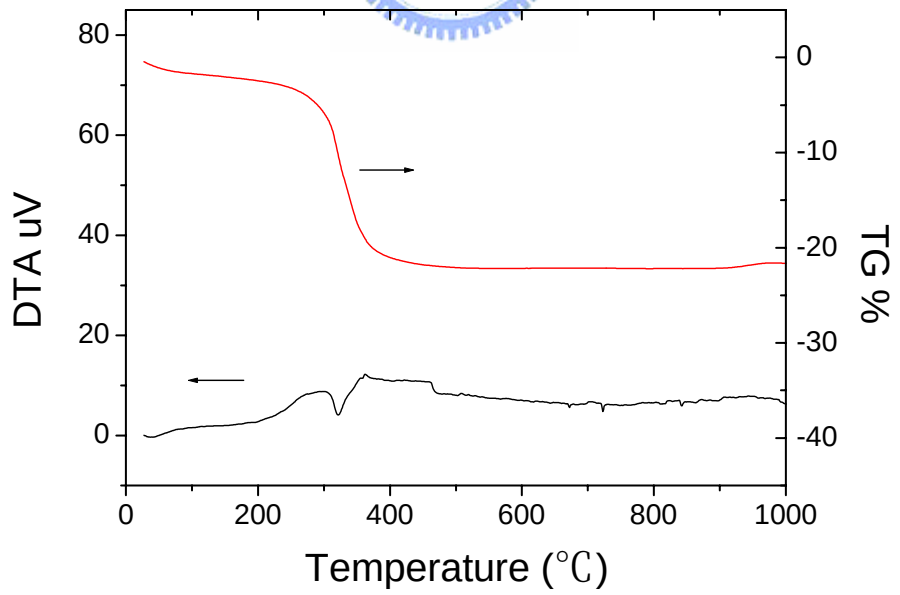

Fig.4-1 DTA and TG curves of the dried powder obtained from the precursor solution.

The XRD patterns shown in Fig. 4-2 reveal that well crystallized SBT phase was obtained for the films with x≧0.2, which shows strong (115) reflection. It shows the second phase, pyrochlore Phase, existed in the films with x=0. Similar result was also observed by Boyle et al. [95,99] that the sample containing the smaller Bi content appeared to be nearly single pyrochlore phase as seen by the very broad diffraction peak at ~34° 2θ and a very small amount of the SBT perovskite phase. It also appeared that Sr deficiency was compensated by excess Bi, owing to Sr^{+2} ionic radius being nearly same as Bi^{+3} ionic radius (Sr^{2+}=1.4Å, Bi^{3+}=1.3Å). The lattice constant decreases with increasing bismuth content as shown in Figure 4-3.

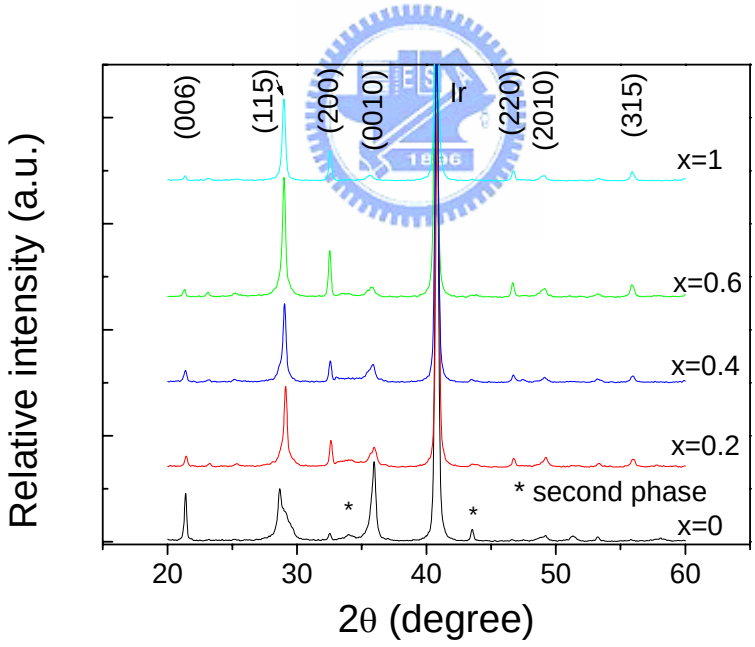

Fig 4-2 XRD patterns of the various bismuth content $Sr_{0.8}Bi_{2+x}Ta_2O_{9+\delta}$ thin films.

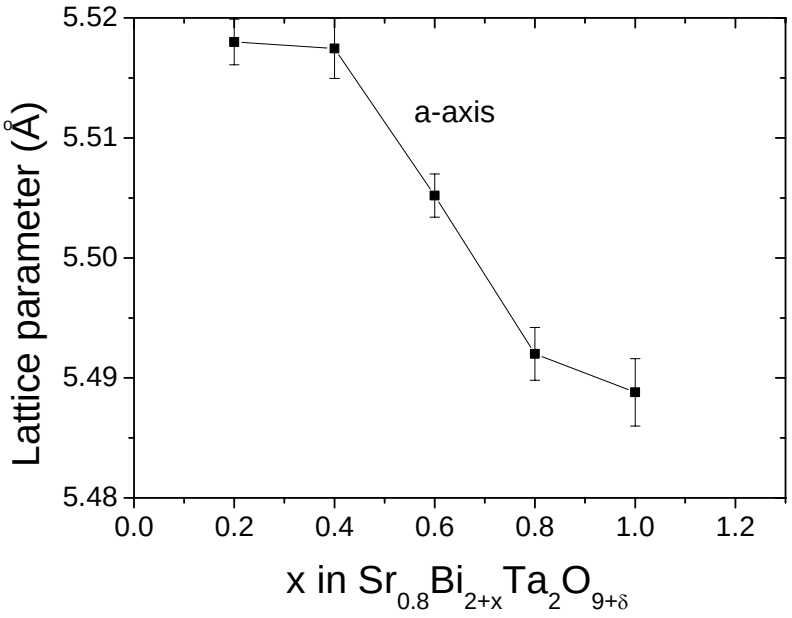

Fig 4-3 Lattice constant of $Sr_{0.8}Bi_{2+x}Ta_2O_{9+\delta}$ films as a function of excess bismuth.

SEM observation of SBT films shows a strong dependence of the composition on the microstructure of SBT films. The morphologies of $Sr_{0.8}Bi_{2+x}Ta_2O_{9+\delta}$ (x=0.4, 0.6, and 1) thin films (Fig.4-4) exhibit very smooth surfaces and no second phase, which are consistent with the result of XRD (Fig.4-2). We need to consider where the excess bismuth possibly goes. In general, one way is to displace Sr site, another way is evaporation of bismuth from the film, and the third way is precipitation of Bi_2O_3 from $Sr_{0.8}Bi_{2+x}Ta_2O_{9+\delta}$ thin films. From the X-ray diffraction patterns and SEM surface images, there appear to be no precipitated second phase such as Bi_2O_3 even though the bismuth contains over 50%.

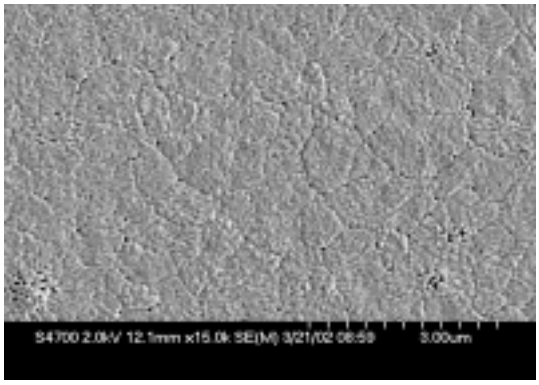

(a) x=1

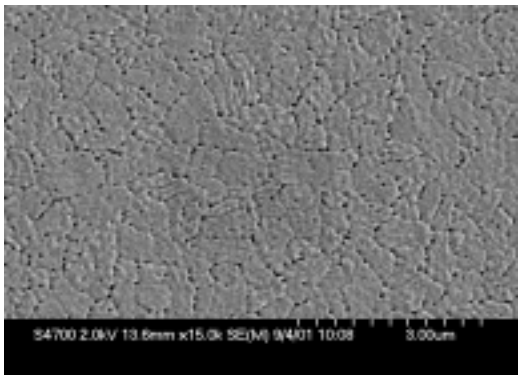

(b) x=0.6

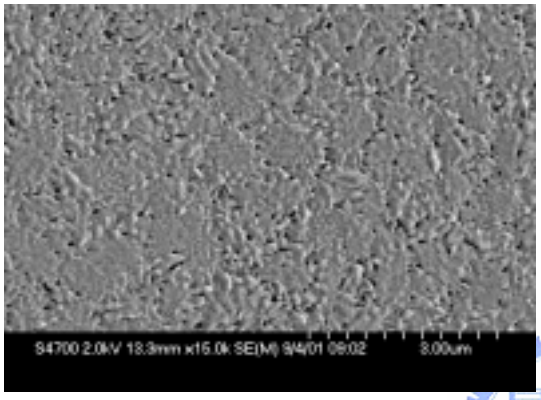

(c) x=0.4

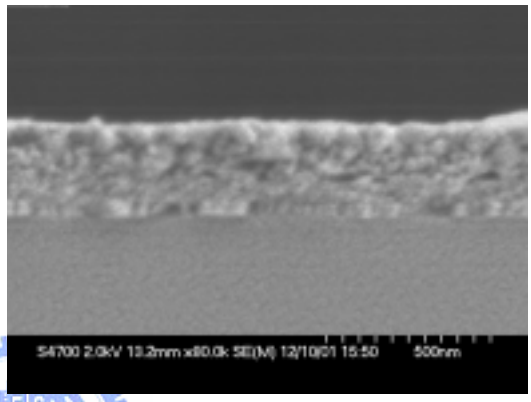

(c) x=0.6

Fig 4-4 SEM micrographs for 650℃, 30 min sintered $Sr_{0.8}Bi_{2+x}Ta_2O_{9+\delta}$ thin film with various excess bismuth content indicated.

Figure 4-5 shows the bismuth (Bi) XPS spectra of SBT thin films with various bismuth contents. The peak intensities at binding energies of approximately 159 and 165 eV, correspond to Bi_2O_3. Figure 4-5 shows the corresponding Bi_2O_3 peak in SBT thin films with bismuth above 30% (x>0.6). The peak intensity at binding energy of approximately 168 and 162.5 eV, which corresponds to Bi_xO_y, is also observed in SBT thin films with no excess bismuth (x=0) content. The peaks corresponding to thin films with bismuth excess less than 10% (x=0.2) shift to higher binding energy with broadening. The chemical shift to higher binding energy of major Bi 4f peak (Bi_xO_y) suggests the existence of bismuth in the (+3-x)

valence state. The chemical shift to higher binding energy with decreasing bismuth excess content may be owing to the difference in bismuth site ratio. Miura and Tanaka [100] investigated the substitution of Bi ions at the Sr site in the Sr-deficient and Bi-excess SBT thin film. The Sr ions in SBT do not have covalent interaction with the surrounding O ions, while the substituted Bi ions at the Sr site do. It was also revealed that the lattice parameter of SBT decreased with bismuth content, that is, Sr deficiency was compensated by excess Bi owing to Sr ionic radii being nearly the same as Bi radii (Sr^{2+}=1.4A, Bi^{3+}=1.3A). Due to the covalent interaction, the Bi ions rather than the Sr ions favor substitution at the Sr site. There is a possibility of compensation due to the change in Bi ion valency (+3-x) at Sr site. The Bi (+3-X) formal oxidation state can be generated due to a deficiency in oxygen and an enhanced concentration of oxygen vacancies in the vicinity of bismuth element, either in the perovskite lattice structure or in the Bi_2O_3 layer. The presence of oxygen vacancies has a significant influence on the fatigue properties of SBT thin films. We observed the remarkable increase of the switching charge of SBT thin films with bismuth excess 10% (x=0.2) for polarization reversal over 10^8 cycles (Fig.4-8). This phenomenon also was observed by Dimos et al. [101], Wu et al [102] and Okamura et al. [103]. Many researches have shown that the fatigue in SBT films arise due to electric charge trapping at domain boundaries and interfaces between films and electrode. The large deviation of the surface composition from the standard composition also probably enhances the leakage current density. Figure 4-7 also shows higher leakage current density for SBT thin film with bismuth excess 10% (x=0.2). However, the wake-up phenomenon does not improve the electrical properties because the capacitors to exhibit a rapid increase in

leakage current. From the P-E hysteresis curve, the polarization of SBT thin films with bismuth excess 10% (x=0.2) is smaller than other ferroelectric.

Figure 4-6 depicts the ferroelectric hysteresis loops of $Sr_{0.8}Bi_{2+x}Ta_2O_{9+\delta}$ films recorded with –10 to +10 V excitations. It shows good ferroelectricity except for x=0.2 film. These results also indicate the substitution of Sr by Bi leads to improve polarization properties.

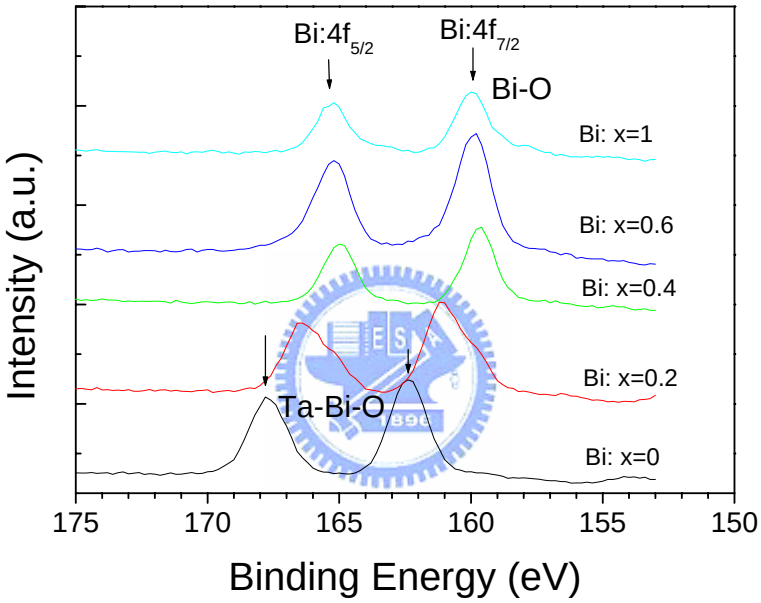

Fig. 4-5 Bi XPS signals of SBT films with various excess bismuth contents.

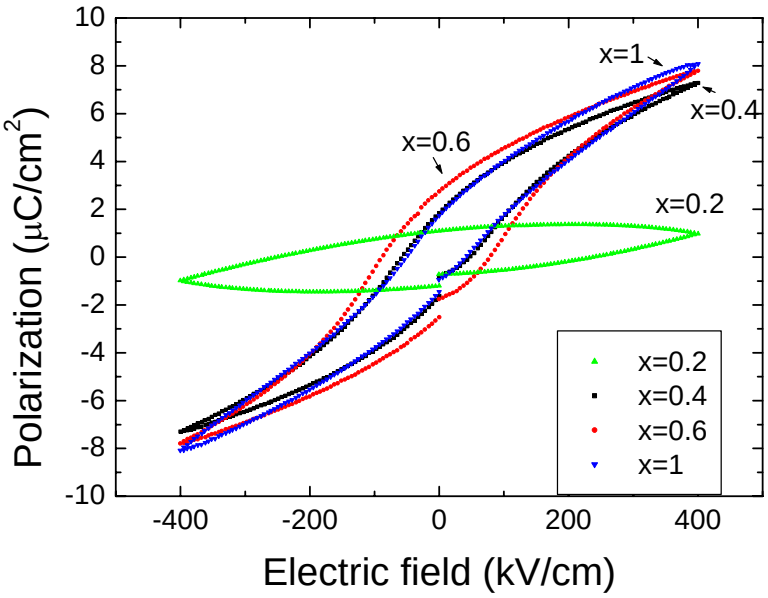

Fig 4-6 P-E hysteresis loops of 650℃, 30 min sintered $Sr_{0.8}Bi_{2+x}Ta_2O_{9+\delta}$ thin films with varying excess bismuth x.

Figure 4-7 displays the leakage current density characteristics of $Sr_{0.8}Bi_{2+x}Ta_2O_{9+\delta}$ thin films. The leakage current density decreases with increasing excess bismuth up to x=0.6, but x=1 film exhibits higher leakage current. The $Sr_{0.8}Bi_{2+x}Ta_2O_{9+\delta}$ thin films with x=0.6 has a low leakage current density of 10^{-7} A/cm^2 at 100 kV/cm. It was reported that the Bi-deficient films had larger leakage current than the Bi-excess films, which was in agreement with the present results for x≦0.6 films [104]. However, why the x=1 film has higher leakage current than x=0.6 film？ It might be due to minor second phase at the grain boundaries. Further TEM study is required to verify the presence of such minor second phase. Figure 4-9(a) shows the TEM planar view micro-morphology of SBT thin film with bismuth excess 50% (x=1). The picture shows the minor second phase among the grain boundary and surface. The minor second phase was

analyzed by EDS, which was the Bi_xTa_y metal complex. It is the Bi_xTa_y complex which leads to the higher leakage current density. That is, the SBT thin film with excess bismuth (x=1) would lead to bismuth co-precipitation with tantalum and lead to higher leakage current density.

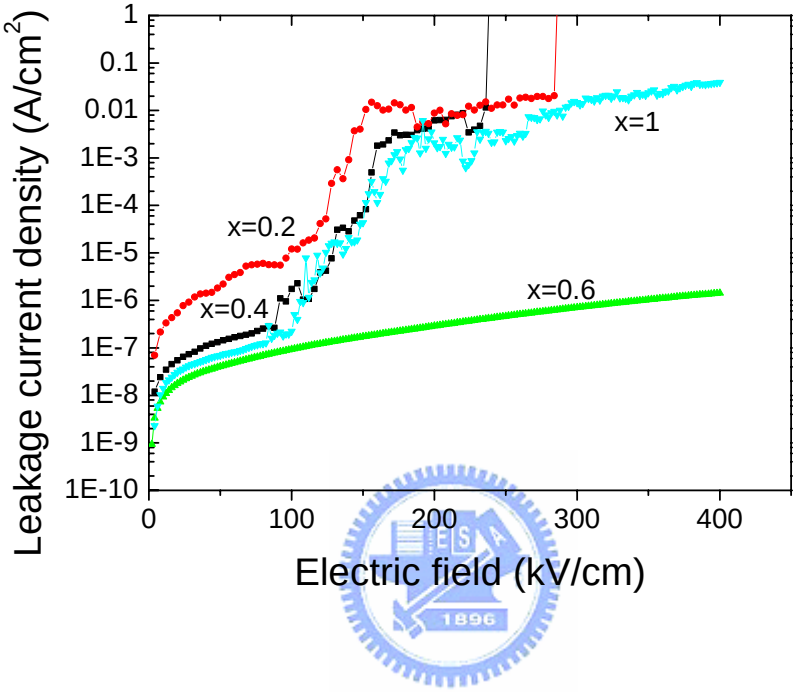

Fig 4-7 Leakage current density vs. applied electric field for $Sr_{0.8}Bi_{2+x}Ta_2O_{9+\delta}$ thin films with various excess bismuth indicates.

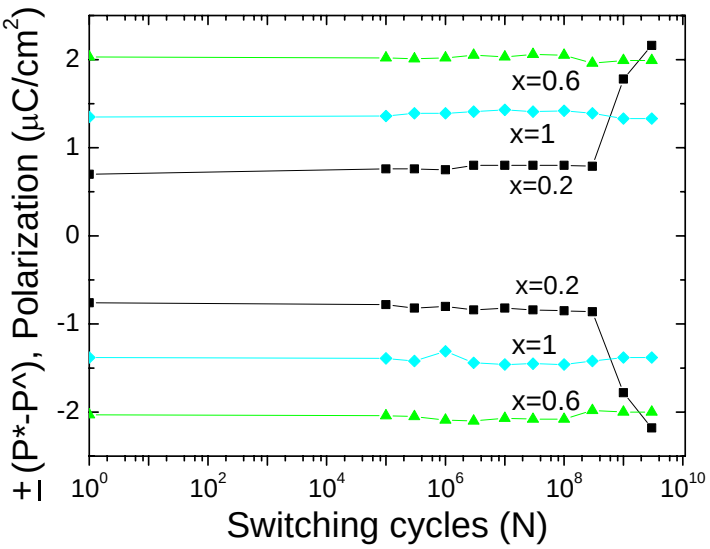

Fig. 4-8 Fatigue characteristics of SBT thin films with various excess bismuth contents annealed at 650℃ under 5V bipolar switching cycles.

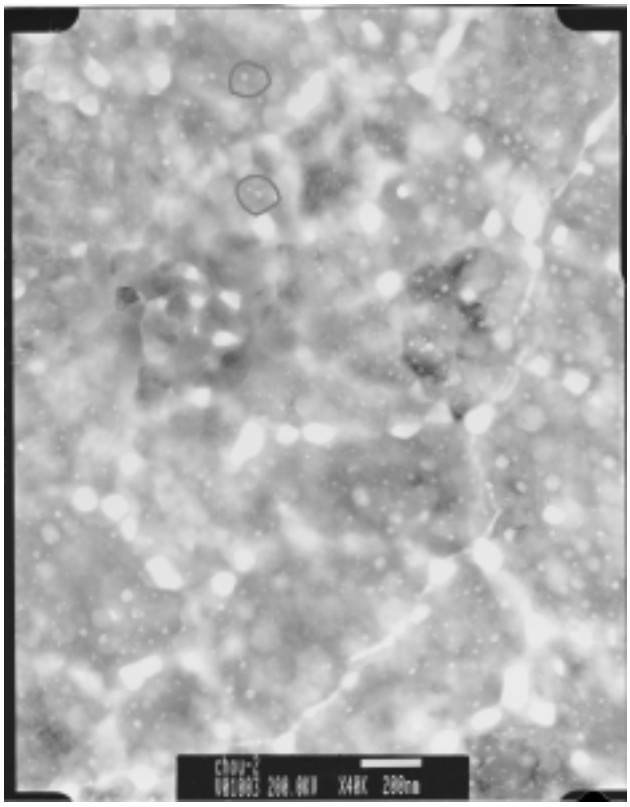

(a)

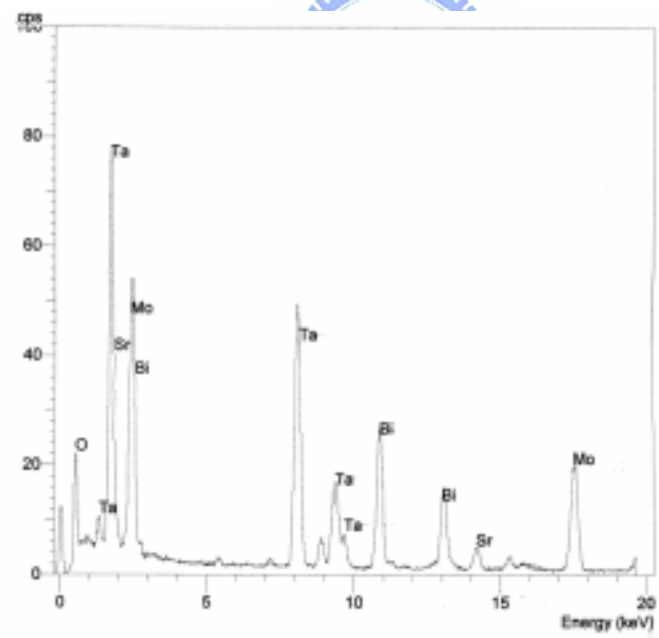

(b)

Fig. 4-9 (a) The TEM image of SBT thin film with excess bismuth 50% (x=1) (b) EDS spectra acquired from minor second phase (marked as black circle in TEM picture) of SBT thin film.

From the above result, the excess bismuth either can substitute Sr site or precipitate along grain boundaries at higher excess amounts. The third way of distribution of excess Bi is evaporation and diffusion to bottom electrode. Figure 4-10 is the SIMS depth profile with 30% (x=0.6) bismuth content of as-deposited and sintered SBT films at 650℃, 700℃ for 30 min. Figure 4-10(b) and 4-10(c) show that the small amounts of bismuth had diffused to the interface between Ir and SBT thin films. It also shows that the amount of bismuth diffusing into bottom electrode increase with increasing temperature. That is, the excess bismuth would have either diffused to the bottom electrode or evaporated from the sample. Though the excess bismuth would evaporate, diffuse and co-precipitate, the SBT thin films with bismuth excess 20%-50% (x=0.4-1) still could maintain the stoichiometric composition. That is the SBT phase and ferroelectricity of SBT thin films can be observed very well.

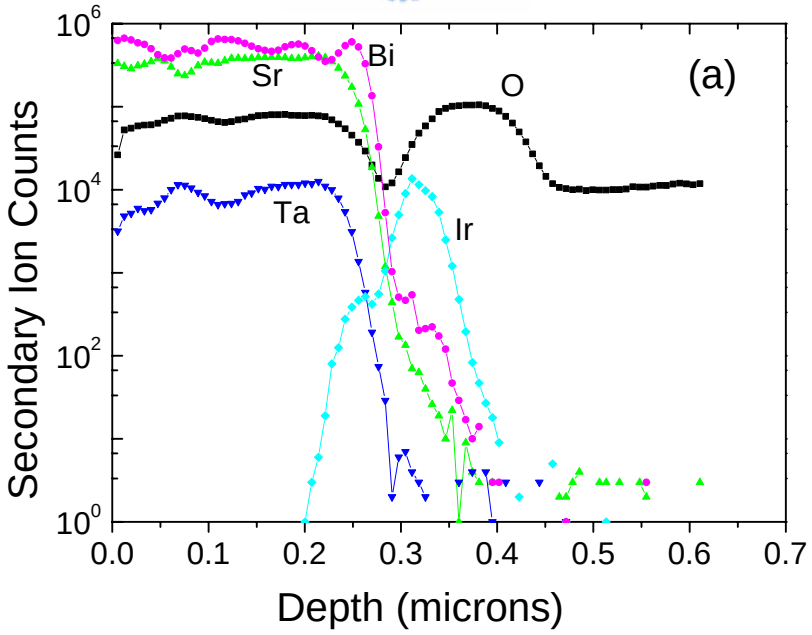

Fig. 4-10(a) SIMS depth profiles of SBT thin films as-deposited.

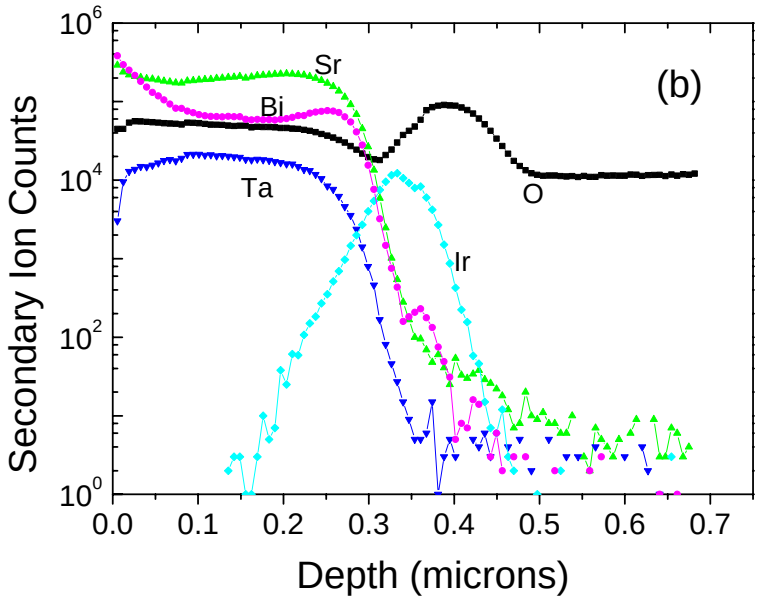

Fig. 4-10(b) SIMS depth profiles of SBT thin films annealed at 650℃, for 30 min.

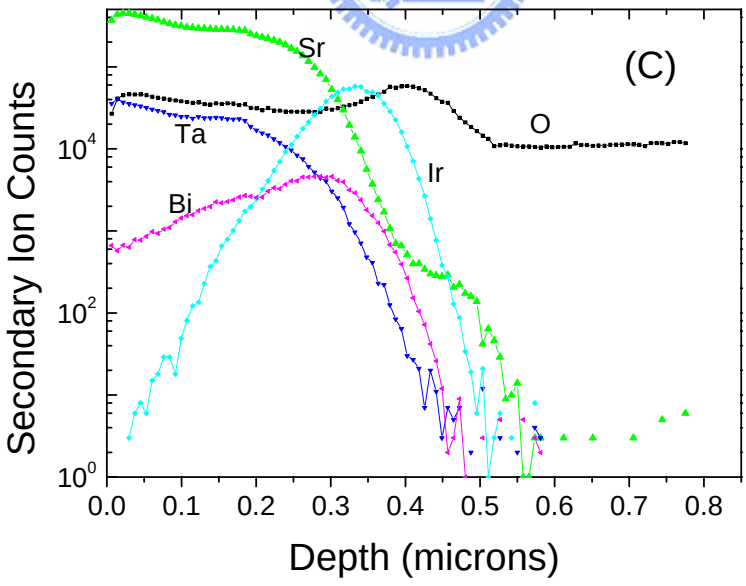

Fig. 4-10(c) SIMS depth profiles of SBT thin films annealed at 700℃, for 30 min.

Figure 4-11 and 4-12 are the plots of ln(J/E) versus $E^{1/2}$, from which we can obtain the electronic conduction mode of SBT thin film capacitors. The electronic conduction current of SBT thin films capacitors is the ohmic conduction in an electric field lower than 100kV/cm but thin film with bismuth excess equal to30 % (x=0.6), the ohmic conduction is the responsible conduction mechanism under even higher electric field. The films, except for the one with bismuth excess equal to 30% content, have shown conduction behavior attributable to Poole-Frenkel emission in an electric field higher than 100kV/cm as shown in figure 4-12.

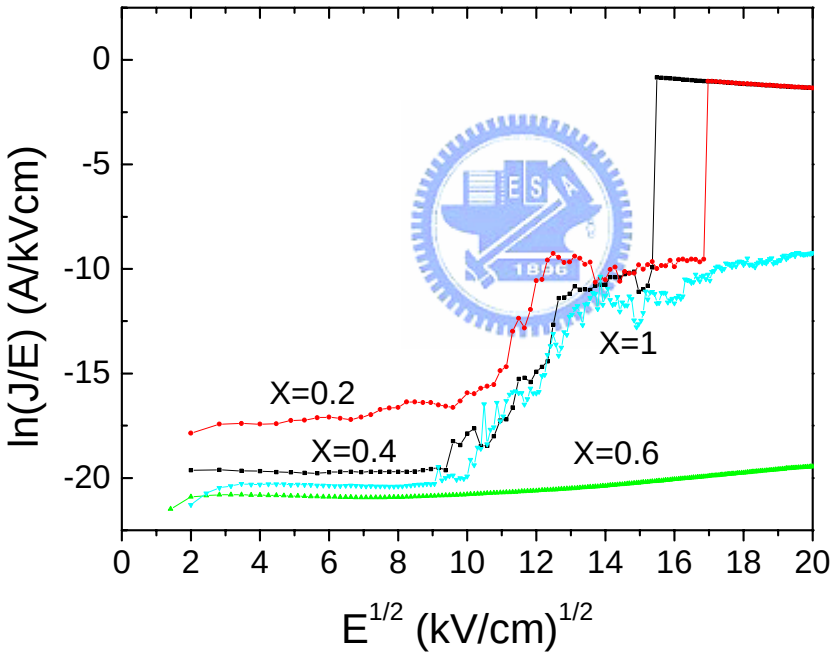

Fig. 4-11 Ln (J/E) is plotted versus $E^{1/2}$ for SBT films with various excess bismuth contents.

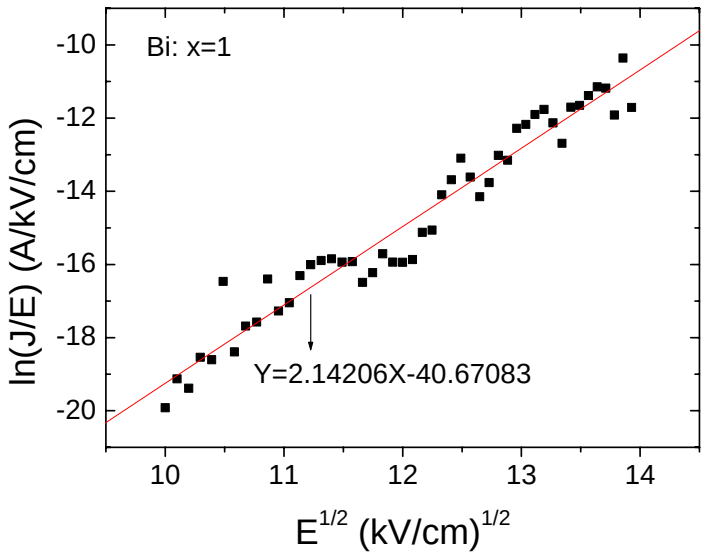

Fig. 4-12 Ln (J/E) is plotted versus $E^{1/2}$ for SBT films with Bi excess x=1.

4-4 Summary

The $Sr_{0.8}Bi_{2+x}Ta_2O_{9+\delta}$ thin films were synthesized on Ir(50nm)/ SiO_2(100nm)/Si substrates using MOD method. A well-crystallized single phase film was obtained by sintering the spin-on films with $x \geqq 0.2$ at 650℃ for 30 min in ambient oxygen atmosphere. The $x \geqq 0.4$ films showed a good ferroelectric property, while the x=0.6 film had a low leakage current density of 10^{-7} A/cm^2 at 100 kV/cm. The excess bismuth substituted the Sr site in the Sr-deficient and Bi-excess SBT thin films. There is a possibility of compensation due to the change in Bi ion valency (+3-x) at the Sr site as the substitution occurs. The leakage current density of SBT thin films with various bismuth contents decreased with increasing bismuth excess up to x=0.6, but x=1 film exhibited higher leakage current. The reduction in leakage current was attributed to the minor second phase Bi_xTa_y complex, which was identified using a TEM-EDS analysis of the sample.